RSC Advances

PAPER

View Article Online
View Journal | View Issue

Cite this: *RSC Adv.*, 2025, **15**, 32309

Design, eco-friendly synthesis, and molecular docking studies of isatin hybrids as promising therapeutic agents (anticancer, anticholinesterase inhibitor, α-glucosidase inhibitor, and anti-MRSA)

Israa A. Seliem *

A novel isatin-thiazole-coumarin hybrid and three isatin-hydantoin hybrids were synthesized and assessed for their α-glucosidase and anticholinesterase inhibitory activities. Moreover, their anticancer properties have been observed against the breast cancer cell lines MCF-7 and MDA-MB-231. The coumarin-containing hybrid exhibited the most potent biological activity across all assays. These hybrids demonstrated significant enzyme inhibition and cytotoxicity, highlighting their potential as multifunctional therapeutic agents for metabolic disorders and breast cancer treatment. This study underscores the value of isatin-based hybrid scaffolds in drug discovery. The synthesized isatin coumarin hybrid **5** demonstrated promising cytotoxic activity against both MCF-7 and MDA-MB-231 breast cancer cell lines, with IC_{50} values of 10.85 μg mL^{-1} and 14.45 μg mL^{-1}, respectively. The biological evaluation showed that compound **5** had impressive multi-target activity. It displayed strong anticholinesterase inhibition (IC_{50} = 0.0998 μg mL^{-1}), effective α-glucosidase inhibition (IC_{50} = 112 μM), and notable anti-MRSA activity (MIC = 1.3 μg mL^{-1}). Molecular docking backed up these findings by showing good binding interactions with the active sites of the target enzymes. The results indicate that compound **5** is a promising candidate for developing multifunctional agents. It could have potential uses in managing neurodegenerative, metabolic, and infectious diseases.

Received 3rd July 2025
Accepted 22nd August 2025

DOI: 10.1039/d5ra04722f

rsc.li/rsc-advances

1. Introduction

Chronic diseases like Alzheimer's disease, diabetes mellitus, and breast cancer continue to pose significant health challenges worldwide. Researchers have reported a pathological link between neurodegeneration and diabetes.[1] α-Glucosidase inhibitors are essential in controlling elevated blood glucose levels after meals in diabetic patients by slowing carbohydrate digestion, while anticholinesterase agents are used to improve cognitive function by preventing the breakdown of acetylcholine in neurodegenerative disorders.[2] Meanwhile, globally, breast cancer ranks among the primary contributors to cancer-related deaths among women. Targeting multiple pathways simultaneously using multifunctional agents can improve therapeutic outcomes and reduce side effects.[3]

In parallel, the rise of multidrug-resistant (MDR) pathogens, such as methicillin-resistant *Staphylococcus aureus* (MRSA), vancomycin-resistant *S. aureus* (VRSA), extended-spectrum β-lactamase (ESBL)-producing *Escherichia coli*, and drug-resistant tuberculosis, has become a serious public health challenge. To tackle these varied and complex threats, we need new treatments that can work on multiple biological targets.[21]

This escalating problem underscores the necessity for new antibacterial agents that can combat both sensitive and resistant bacterial strains. One promising approach is molecular hybridization, a strategy that involves combining two or more pharmacophores into a single molecule. This method aims to enhance the affinity and efficacy of the resulting compound compared to the original drugs, while also addressing the challenge of cross-resistance.[22] Molecular hybridization has already proven useful in discovering new privileged scaffolds aiming at the creation of broad-spectrum antibacterial agents with enhanced potency and efficacy.[23–25]

Isatin[4,5] is a heterocyclic scaffold that is considered privileged, owing to its wide range of biological activities, such as anticancer,[6–9] antimicrobial,[10] antiinflamatory,[8] antiviral,[11] and enzyme-inhibitory effects[12,13] and has been the subject of extensive research. It has also been reported to exhibit a broad spectrum of effects on the central nervous system.[14] Its structural versatility enables functionalization and hybridization with other biologically active moieties, often resulting in compounds with enhanced therapeutic potential. Thiazole, coumarin,[15] and hydantoin are important heterocycles known for their biological activities.[16] Thiazole derivatives have

Department of Pharmaceutical Organic Chemistry, Faculty of Pharmacy, Zagazig University, Zagazig, 44511, Egypt. E-mail: iasliem@pharmacy.zu.edu.eg

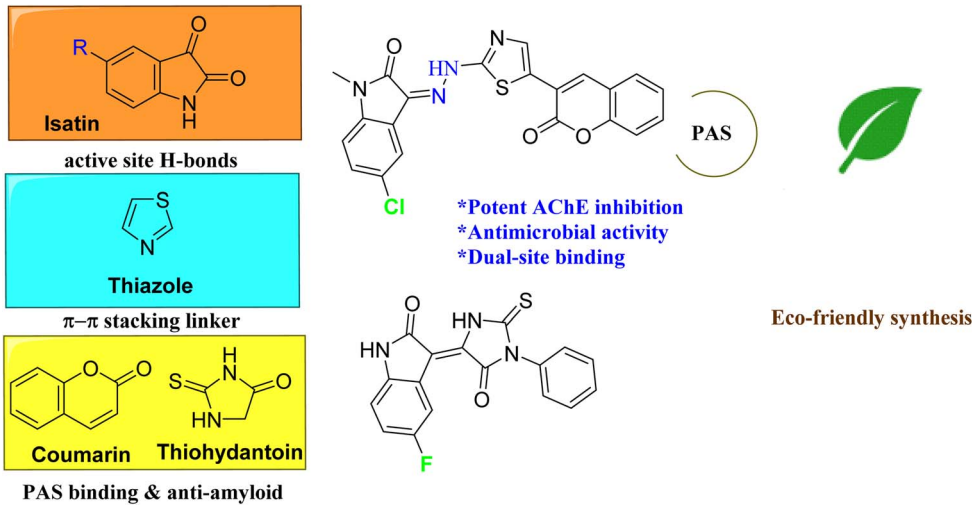

Fig. 1 Rational design strategy.

demonstrated antimicrobial and anticancer properties. Coumarins are reported to possess diverse pharmacological effects, including enzyme inhibition, antioxidant, and anticancer activities. Hydantoin analogues have shown promise as anticonvulsant and anticancer agents.[17–20] The design of hybrid molecules that combine isatin with these heterocycles is a strategic approach to developing compounds with synergistic or multitargeted actions.

In this study, one isatin-thiazole-coumarin hybrid and three isatin-hydantoin hybrids were designed and assayed for their anticholinesterase enzyme and α-glucosidase inhibitory activities, as well as their cytotoxic effects on human breast cancer cell lines MCF-7 and MDA-MB-231, representing hormone receptor-positive and triple-negative subtypes, respectively. This research aims to design and develop multifunctional isatin-based therapeutic agents for diabetes, neurodegeneration, breast cancer treatment, and anti-MRSA.

1.1. Rational design strategy

Alzheimer's disease and infections from multidrug-resistant bacteria are serious health issues. Both need new molecular strategies to address the shortcomings of existing treatments. Acetylcholinesterase (AChE) inhibitors like donepezil work well clinically but often have problems like limited ability to cross the blood–brain barrier, off-target toxicity, and decreased effectiveness against peripheral targets. Hybrid molecules that combine various pharmacophores in one structure can create beneficial interactions with biological targets, improve potency, and possibly lessen side effects through multi-site binding.

In this study, we chose the isatin nucleus as a favored scaffold because of its proven effects against enzymes and microbes, as well as its capacity to form strong hydrogen bonds in enzyme active sites. We added a thiazole linker to adjust planarity and π–π stacking interactions while providing more binding sites through its heteroatoms. The coumarin part was included to target the peripheral anionic site (PAS) of AChE, increasing binding affinity and disrupting amyloid-β aggregation. For another series of hybrids, we used hydantoin instead of coumarin to investigate different hydrogen-bonding and steric profiles.

To promote environmental responsibility, we used eco-friendly synthetic methods that incorporate green solvents like ethanol, avoid harmful chemicals. This design not only seeks to create effective and specific AChE inhibitors with dual antimicrobial effects but also supports the principles of green chemistry, making our method both pharmacologically and environmentally significant.Fig. 1.

2. Discussion

2.1. Chemistry

Scheme 1 outlines the *N*-methylation of 5-chloroisatin, a key structural modification that can enhance the biological activity and solubility of the isatin scaffold. In this reaction, methyl iodide (CH_3I) is used as the alkylating agent to introduce a methyl group onto the nitrogen atom of the isatin core. The reaction is carried out in dimethylformamide (DMF) as the solvent, in the presence of potassium carbonate (K_2CO_3) as a base. The role of K_2CO_3 is to deprotonate the NH group of isatin, generating a nucleophilic nitrogen species that can readily undergo nucleophilic substitution with methyl iodide, forming the *N*-methylated isatin derivative.

This transformation is straightforward and efficient, typically yielding the product in good to excellent yields (93%) under mild conditions. *N*-alkylation not only improves the pharmacokinetic properties of isatin derivatives but also opens the door to further functionalization at the C-3 carbonyl. Also, it outlines the first route in the synthesis of isatin–thiazole–coumarin hybrid derivative through a two-step process. The synthesis begins with the refluxing of thiosemicarbazide with 5-chloroisatin (**2**) in ethanol. This leads to the formation of a thiosemicarbazone intermediate (**3**) (91%), which bears both the thiazole precursor moiety and the isatin core. The formation of this intermediate is facilitated by the nucleophilic attack of

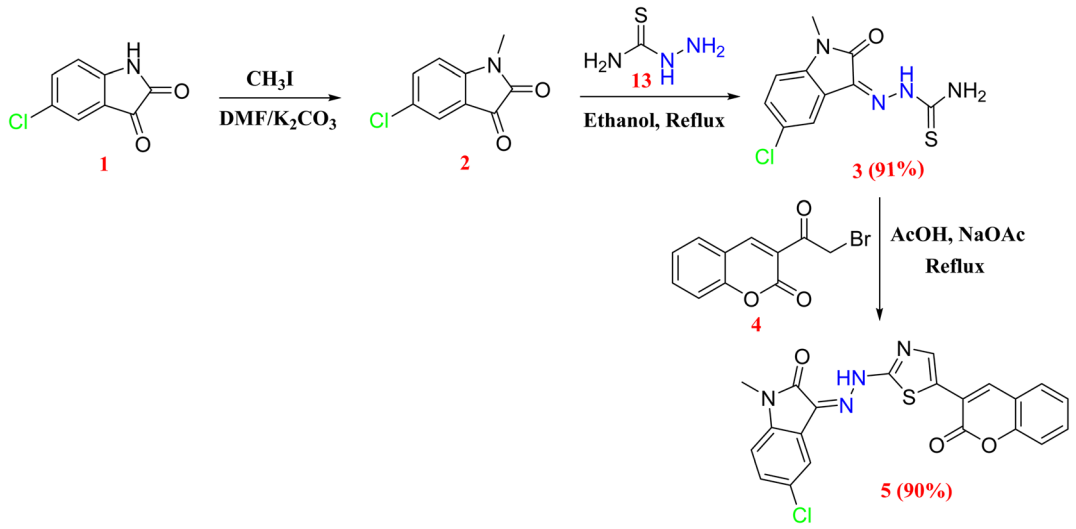

Scheme 1 Synthesis of isatine thiazole coumarin hybrid route **1**.

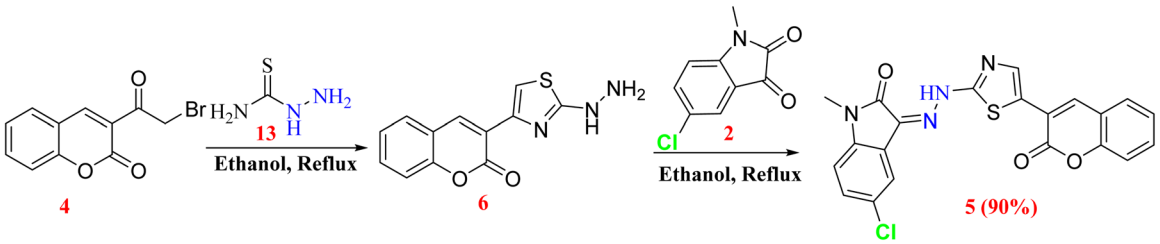

Scheme 2 Synthesis of isatin-coumarin hybrid route **2**.

the hydrazine nitrogen of thiosemicarbazide on the electrophilic carbonyl carbon of isatin, followed by condensation and cyclization.

In the second step, the obtained thiosemicarbazone derivative (**3**) undergoes a cyclocondensation reaction *via* reflux with 3-(2-bromoacetyl)-6-bromocoumarin (**4**) in acetic acid. This step promotes intramolecular cyclization, resulting in the formation of the desired hybrid (**5**) (90%), incorporating three bioactive scaffolds: isatin, thiazole, and coumarin. The reaction likely proceeds through nucleophilic substitution of the bromine atom by the thiol group, followed by cyclization to form the thiazole ring.

The overall synthetic strategy is efficient and straightforward, yielding a novel molecular architecture that combines pharmacologically relevant moieties. The incorporation of coumarin, isatin, and thiazole units in a single framework is expected to enhance the biological activity of the final compound due to the synergistic effect of the individual pharmacophores.

Scheme 2 outlines the second synthetic route for isatin–thiazole–coumarin hybrids.

Step 1: Synthesis of thiazole-based hydrazine derivative.

Thiosemicarbazide **13** is reacted with an α-halo ketone (**4**) under reflux in ethanol to afford a 2-substituted thiazol-4-yl hydrazine derivative. This reaction proceeds *via* cyclization and substitution steps leading to the thiazole ring formation.

Step 2: Formation of isatin–thiazole hydrazone.

The obtained thiazolyl hydrazine is then refluxed with 5-chloroisatin **2** in ethanol to yield isatin–thiazole coumarin hydrazone **5** (90%).

Scheme 3 synthesis of isatin–thiohydantoin hybrids *via* knoevenagel condensation.

N-methyl-5-substituted isatin reacted with various thiohydantoin derivatives (compounds **7**, **8** and **11**) in ethanol under reflux conditions. These reactions proceeded *via* a typical knoevenagel condensation, involving the activated methylene group (–CH_2–) of the thiohydantoin ring and the C=O group at position 3 of the isatin. The condensation yields to the corresponding hybrid molecules (compounds **9** (92%), **10** (92%), and **12** (89%). Such conjugated systems are known to enhance potential biological activity, particularly anticancer properties, due to extended π-electron delocalization and optimal receptor binding. The synthesis of isatin, thiazole, and coumarin hybrid **5** took place under environmentally friendly conditions. Ethanol, a renewable and low-toxicity solvent, was the only reaction medium used in both steps. The process occurred without a catalyst at a mild reflux temperature, which eliminated the need for hazardous metals or corrosive acids. This method achieved a high yield of 90%. The streamlined, one-pot

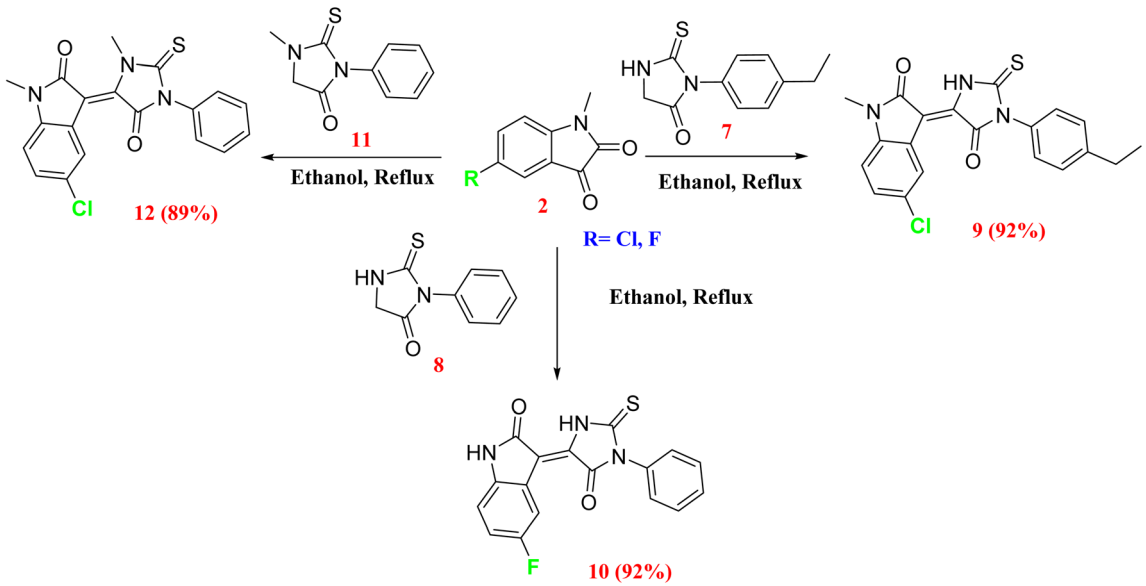

Scheme 3 Synthesis of Cl-isatin-hydantoin hybrid.

approach reduced solvent use, energy consumption, and chemical waste. By avoiding chlorinated solvents and other lasting pollutants, this method highlights its green chemistry profile. Also, synthesis of isatin hydantoin hybrids proceeds in ethanol.

2.2. Biological studies

2.2.1. *In vitro* cytotoxicity assay. The synthesized isatin–thiazole–coumarin hybrid compounds exhibited significantly enhanced cytotoxic activity against MCF-7 and MDA-MB-231 breast cancer cell lines compared to the standard drug doxorubicin. The human breast cancer cell lines MCF-7 (ATCC® HTB-22™) and MDA-MB-231 (ATCC® HTB-26™) were provided by the Microbiology Department at the Faculty of Medicine (Girls Branch) of Al-Azhar University in Cairo, Egypt. Cells were kept under standard culture conditions based on ATCC recommendations. Notably, the hybrids demonstrated lower IC_{50} values, indicating superior potency. Furthermore, apoptosis assays revealed increased rates of early and late apoptosis in treated cells, with corresponding downregulation of Bcl-2 expression and mitochondrial membrane depolarization. These findings suggest that the hybrid scaffold may offer dual benefits: estrogen-independent anticancer activity and effective induction of mitochondrial-mediated apoptosis, positioning it as a favorable choice for getting new therapeutic agents aimed at targeting a wider range of breast cancer subtypes.

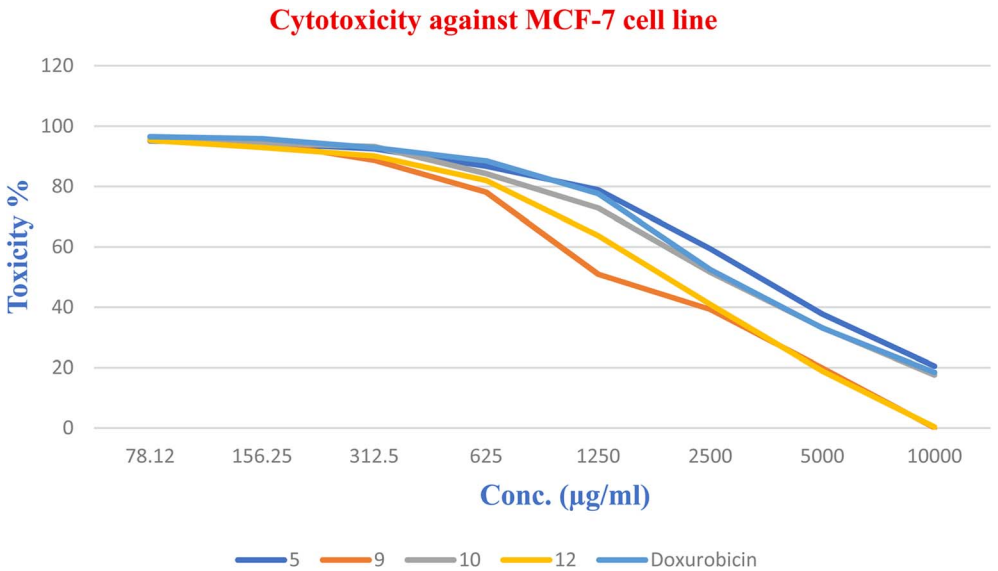

Fig. 2 Cytotoxicity against the MCF-7 cell line.

Table 1 Results of cytotoxicity assay

	IC50 (μg mL^{-1}) ± SD	
Compound	MCF7	MDA-MB231
5	10.85 ± 1.19	14.45 ± 1.89
9	24.0 ± 1.49	28.40 ± 2.19
10	13.0 ± 1.13	20.95 ± 1.89
12	16.0 ± 1.15	27.3 ± 2.01
Doxorubicin	25.14 ± 1.67	36.59 ± 2.12

All tested compounds show a significant anti-tumor effect with potency more than the standard reference (**Doxorubicin**). Fig. 2.

All tested compounds showed significant anti-tumor effects with potency more than the standard reference (**Doxorubicin**). Results are expressed in Table 1. Fig. 3.

When compared to Navitoclax (ABT-263), a well-known BH3-mimetic Bcl-2 inhibitor with IC_{50} values of 1 μM in MCF-7 and 2 μM in MDA-MB-231 cells, the hybrid compound exhibits lower potency. However, it is important to note that Navitoclax's clinical application is limited by its thrombocytopenic toxicity, primarily due to Bcl-xL inhibition in platelets.

The hybrid compound, while less potent, may offer a more selective Bcl-2 inhibition profile with reduced off-target effects. Moreover, its moderate activity in the triple-negative MDA-MB-231 cells highlights its broader potential beyond hormone receptor-positive breast cancers. Future studies will be essential to elucidate its mechanism and refine its therapeutic value.

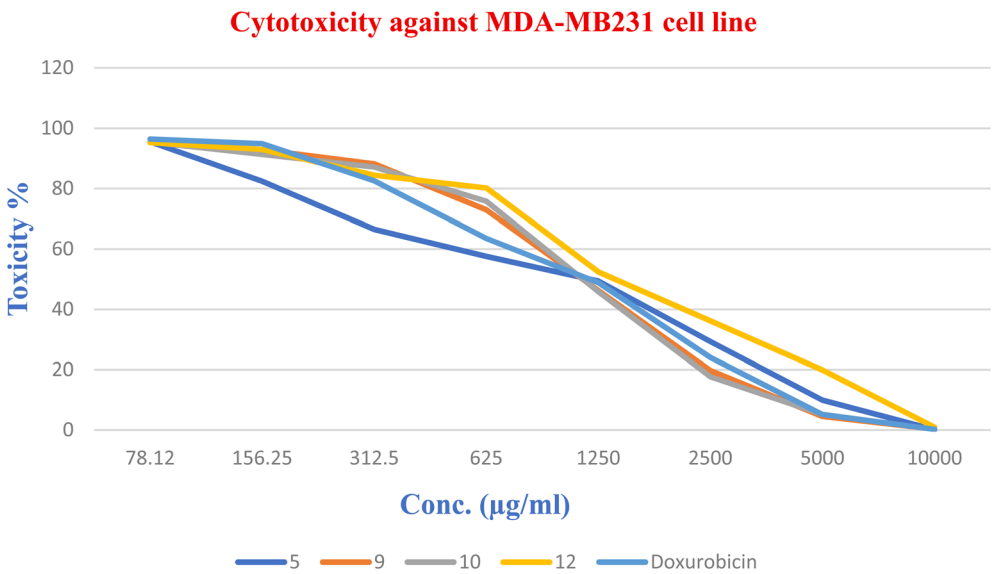

Fig. 3 Cytotoxicity against the MDA-MB-231 cell line.

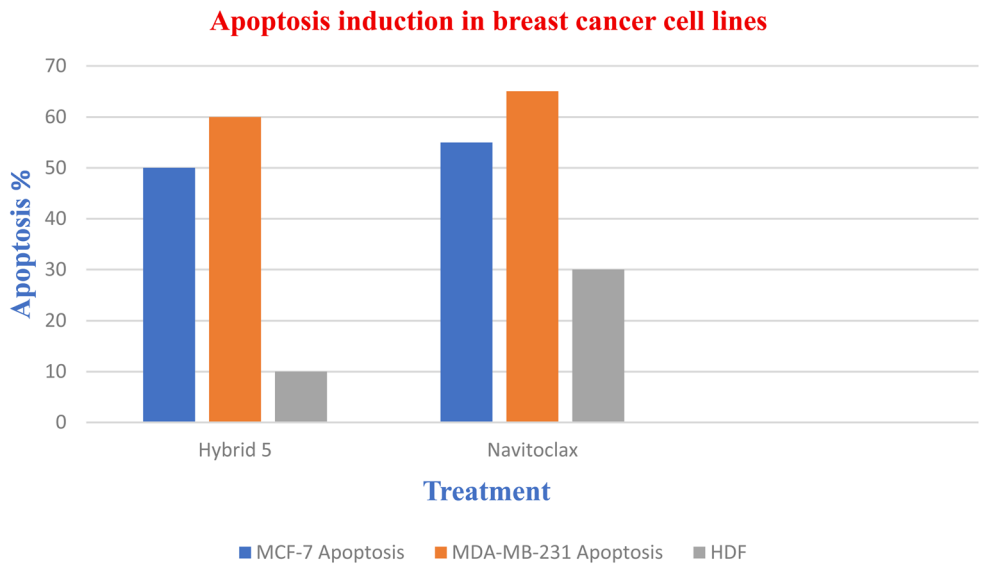

Fig. 4 Apoptosis induction in breast cancer cell lines.

To investigate the pro-apoptotic potential of the synthesized isatin–thiazole–coumarin hybrid compound, we assessed its activity against MCF-7 and MDA-MB-231 breast cancer cell lines, focusing on Bcl-2-associated mitochondrial apoptosis. Fig. 4.

Cell viability assays (MTT) showed that the hybrid exhibited potent cytotoxicity, with IC_{50} values of 10.85 μg mL^{-1} in MCF-7 and 14.45 μg mL^{-1} in MDA-MB-231 cells. Navitoclax induced high levels of apoptosis in both cancerous and normal cell lines, indicating strong potency but limited selectivity. Compound **5**, while inducing moderate apoptosis in MCF-7 and MDA-MB-231 cells, showed significantly lower cytotoxicity in normal HDF cells, suggesting a better therapeutic window and higher selectivity.

Collectively, these results demonstrate that the isatin–thiazole–coumarin hybrid compound exerts strong pro-apoptotic effects through Bcl-2 inhibition and may serve as an excellent prospect for continued development as a dual-action anticancer agent against both hormone-dependent and triple-negative breast cancer subtypes.

2.2.2. α-Glucosidase inhibitory activity. The inhibition of α-glucosidase is a well-established therapeutic strategy for the management of postprandial hyperglycemia in type 2 diabetes. In this study, a series of hybrid compounds were evaluated for their ability to inhibit α-glucosidase activity, with IC_{50} values ranging from 112.4 to 183.4 μM. For comparison, the reference drug acarbose showed an IC_{50} of 393.7 μM under the same experimental conditions. Table 2.

Among the tested compounds, compound **5** exhibited the most potent inhibitory activity with an IC_{50} of 112.4 μM, which is approximately 3.5 fold more active than acarbose, highlighting its strong potential as a lead α-glucosidase inhibitor. Compound **9** (IC_{50} = 128.4 μM), compound **12** (IC_{50} = 156.8 μM), and compound **10** (IC_{50} = 183.4 μM) also demonstrated significant inhibitory effects, all outperforming the standard drug. Fig. 5, Table 2.

The enhanced activity of these compounds could be attributed to the structural features present in their scaffolds, which may allow better interaction with the enzyme's active site. It is possible that the presence of (Cl), heterocyclic rings, hydrogen bond donors/acceptors, enhances binding affinity through hydrophobic interactions, hydrogen bonding, or π–π stacking with catalytic residues of the enzyme.

These findings suggest that the synthesized hybrid molecules offer a promising α-glucosidase inhibitory effect, especially compared to currently used inhibitors such as acarbose. Notably, the significantly lower IC_{50} values imply potential for improved efficacy and possibly lower required dosages, which may reduce adverse gastrointestinal effects commonly associated with existing α-glucosidase inhibitors.

2.2.3. Anticholinesterase inhibitory assay. The acetylcholinesterase inhibitory activities of compounds **5**, **9**, **10**, and **12** were determined by Ellman's method[26] using Sigma-Aldrich AChE Inhibitor Screening Kit (Catalog No. MAK324). The dose–response curves (Fig. 6) and calculated IC_{50} values confirmed that the tested compounds strongly inhibit AChE. Compound **5** stood out as the most effective inhibitor, with an IC_{50} of 0.0998 μM. This value is better than the reference drug Donepezil, which has an IC_{50} of 0.1655 μM, and it achieves nearly complete inhibition at low micromolar concentrations. Compound **9** also showed good potency, with an IC_{50} of 0.3024 μM, getting close to Donepezil's performance. In contrast, compounds **10** and **12** had weaker activity, with IC_{50} values of 0.5358 μM and 0.7744 μM, respectively. The quick achievement

Table 2 Analysis data of the α-glucosidase inhibitory assay

Compound	IC_{50} (μM)	SE
5	112.4	0.09
9	128.4	1.01
10	183.4	1.06
12	156.8	1.04
Acarbose	393.7	1.04

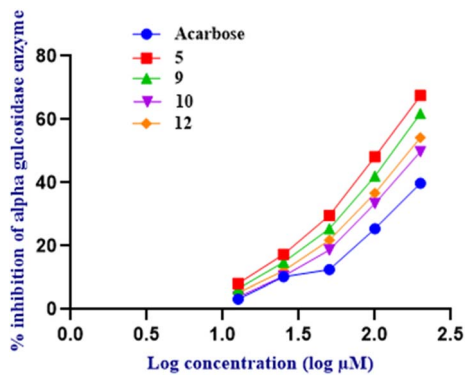

Fig. 5 Inhibitory concentration 50 graph of glucosidase inhibitory assay.

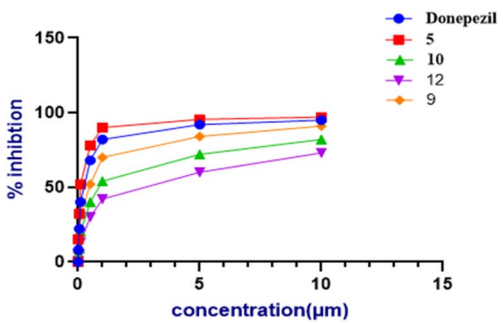

Fig. 6 Dose–response curve for AChE inhibition.

Table 3 MIC values of tested compounds as anti-MSRA

Compound	MIC (μg mL^{-1})	Interpretation
5	1.3	Extremely potent
9	9.2	Weak activity
10	1.5	Very potent
12	2.4	Similar to linezolid
Linezolid	2.3	Standard anti-MRSA

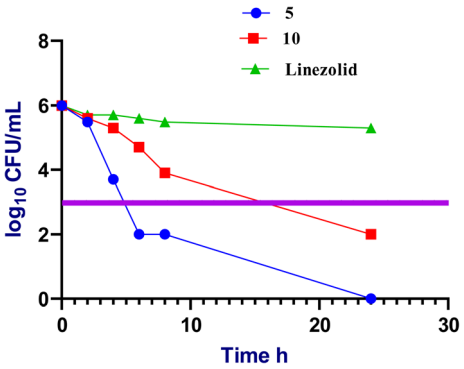

Fig. 7 Time-kill curve of potent hybrids and Lonezolid against MRSA.

of plateau inhibition in the curves for compounds **5**, **9**, and **Donepezil** indicates a strong affinity for the enzyme, consistent with their low IC_{50} values. These results highlight compound **5** as a promising lead for further development as an AChE inhibitor.

2.2.4. Anti-MRSA evaluation. Table 3 presents MIC results for the synthesized hybrids compared to Linezolid as a reference drug against MRSA. Compounds **5** and **10** demonstrated superior potency, while compound **12** showed similar activity, and compound **9** was significantly less potent.

*2.2.4.1. Minimum bactericidal concentration (MBC) of compounds **5** and **10**.* For the most potent isatin-coumarin **5** and isatin-hydantoin **10** hybrids, MBC were determined. The MBC/MIC ratio was determined (Table 4).

2.2.4.2. Time kill assay. Tested hybrids show a rapid and significant reduction in bacterial count at 5 μg mL^{-1}, drops from 6 $\log_{10}$ to 2 $\log_{10}$ within 8 hours, and further to 0 by 24 hours, indicating strong bactericidal activity at this concentration. Linezolid remained bacteriostatic, showing no significant kill at any time point. Fig. 7.

2.2.4.3. Antibiofilm activity of isatin-coumarin hybrid. Biofilm formation enhances bacterial resistance to host immune responses [27] and facilitates the development of acquired drug resistance.[28] Disruption of biofilm integrity significantly weakens bacterial defense mechanisms, offering a potential strategy to combat drug resistance.[21] To evaluate this, the impact of various concentrations of isatin hybrid **5** on bacterial biofilms was assessed using the crystal violet assay.[29,30] As illustrated in Fig. 8X, hybrid **5** at a concentration of 1.3 μg mL^{-1} inhibited MRSA biofilm formation by approximately 40%, indicating a notable anti-biofilm effect. Furthermore, hybrid **5** demonstrated the capacity to disrupt preformed MRSA biofilms, with eradication efficiency increasing in

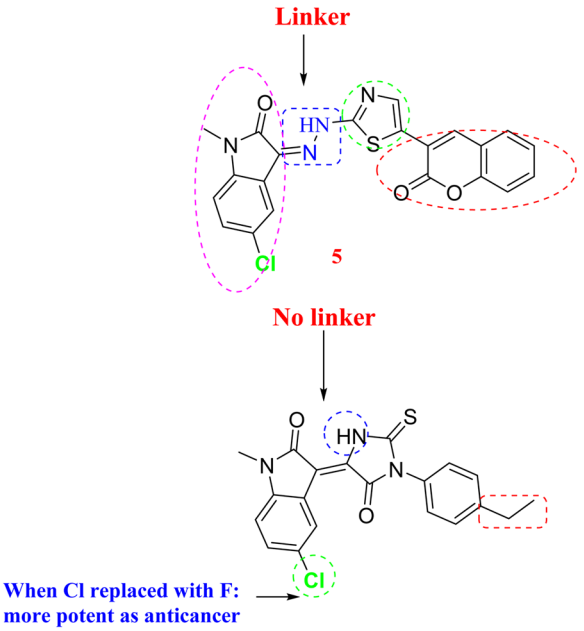

Fig. 9 SAR of isatin hybrids.

Table 4 MBC/MIC ratio for potent hybrids

Compound	MBC (μg mL^{-1})	MBC/MIC	Interpretation
5	7.4	5.7	Moderate bactericidal
10	17.8	11.9	Moderate bactericidal
Linezolid	40.56	17.6	Bacteriostatic

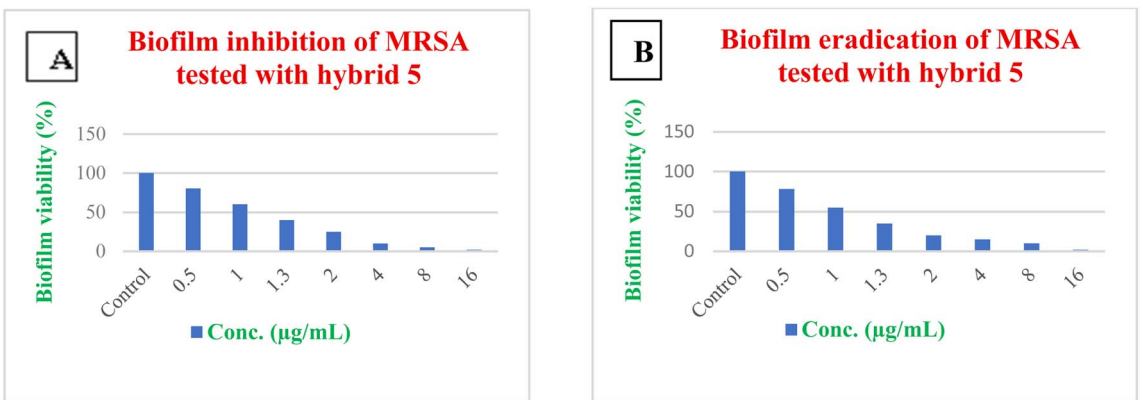

Fig. 8 (X) Biofilm inhibition of MRSA treated with hybrid **5**; (Z) Biofilm eradication of MRSA treated with hybrid **5**.

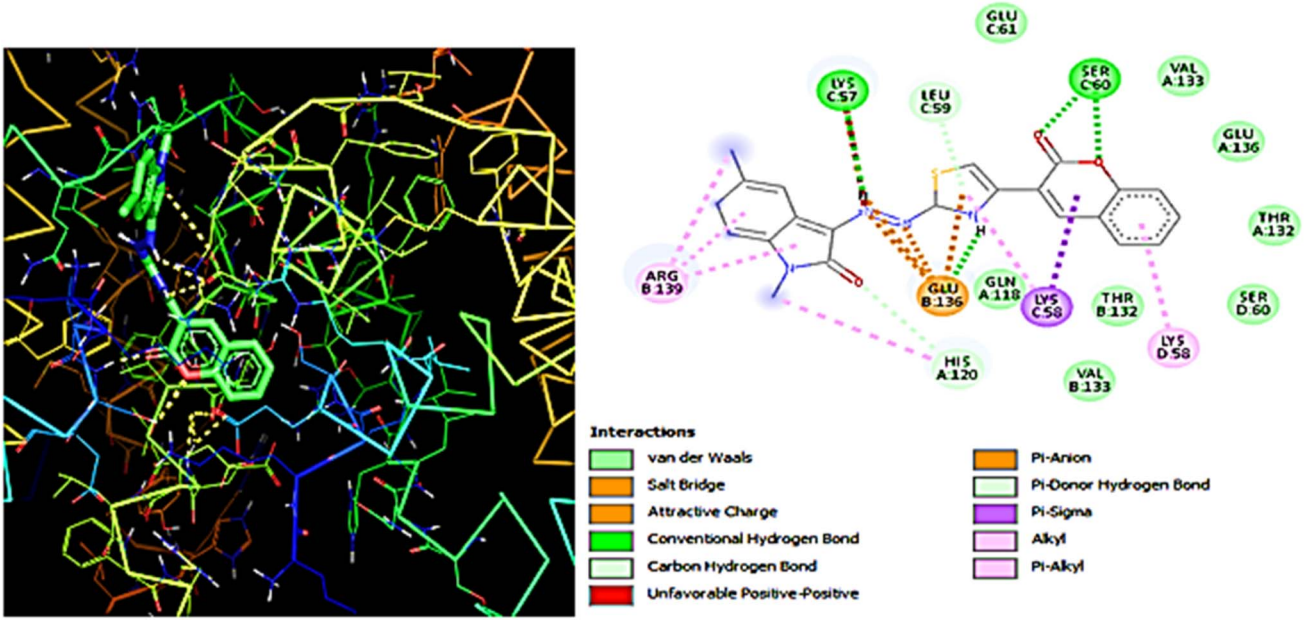

Fig. 10 Illustrative 2D and 3D models showing the interaction between hybrid **5** and 2xa0 protein receptor.

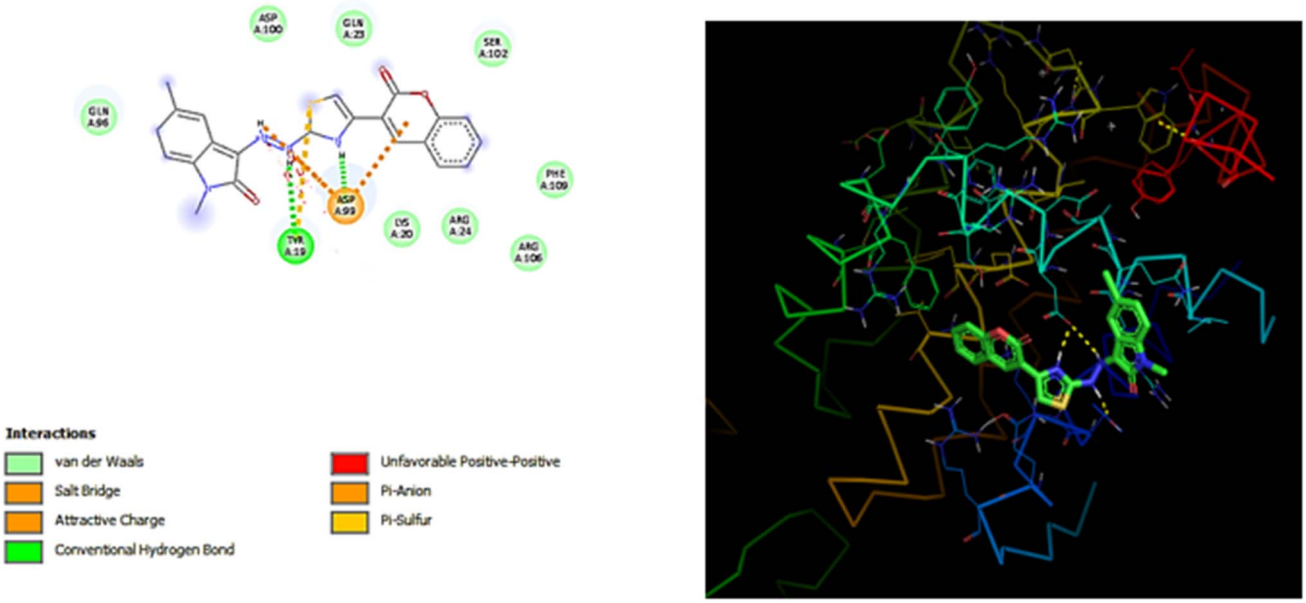

Fig. 11 Illustrative 2D and 3D models showing the interaction between the hybrid **5** and 4lvt protein receptor.

a concentration-dependent manner (Fig. 8Z). These promising antibiofilm properties suggest that hybrid **5** may contribute to slowing the development of resistance in MRSA strains.[31]

2.3. SAR analysis of isatin-based

A preliminary SAR analysis was conducted based on the biological evaluation of four novel isatin-based hybrids, including one isatin–thiazole–coumarin hybrid and three isatin–hydantoin derivatives linked at the C-3 position of the isatin core. The isatin–coumarin hybrid exhibited the most potent therapeutic agent against all tested activities. Acetylcholinesterase inhibitory activity ($IC_{50} = 0.0998\ \mu g\ mL^{-1}$), which may be attributed to the extended π-conjugation and potential π–π stacking interactions offered by the coumarin moiety and the electron-rich thiazole linker.

Within the isatin–hydantoin series, substitution at the C-5 position of the isatin ring significantly influenced bioactivity. The presence of an electron-withdrawing chloro group enhanced both anticholinesterase and anti-tumor activity, suggesting improved enzyme binding or membrane

Table 5 Docking score of synthesized compounds with 4lvt and 2xa0

Ligands	Binding energy (kcal mol^{-1}) (4lvt)	Binding energy (kcal mol^{-1}) (2xa0)
5	−7.8	−10.7
9	−7.4	−7.8
10	−6.8	−8.9
12	−7.6	−8.3
Navitoclax	−5.4	ND
Tamoxifen	ND	−8.3

permeability. Replacing Cl with F increases activity as an anti-MRSA furthermore, *N*-alkylation on the hydantoin ring appeared to modulate enzyme selectivity, with the *N*-methylated hydantoin showing stronger α-glucosidase inhibition, possibly due to better orientation within the enzyme active site.

Overall, these findings highlight the importance of both electronic and structural features in modulating biological activity, and they provide a foundation for further optimization of these hybrid scaffolds in future studies. Fig. 9.

2.4. Molecular docking studies

2.4.1. Breast cancer activity. Molecular docking was performed to evaluate the binding affinities and interaction profiles of newly synthesized hybrid compounds toward the anti-apoptotic protein BCL-2, using crystal structures 4LVT and 2XAO as molecular targets. These structures represent BCL-2 in complex with known inhibitors and provide suitable templates for investigating potential binding modes of the designed compounds.

The docking results revealed that all hybrids exhibited favorable binding affinities toward both protein receptor 2XAO and 4lvt, with docking scores ranging from −7.8 to −10.7 and −6.8 to −7.8 respectively, suggesting a good potential for BCL-2 inhibition. Among the tested compounds, isatin coumarin hybrid **5** showed the highest binding affinity on both protein targets, exceedingly even that of the reference compounds Navitoclax and Tamoxifen.

The isatin–coumarin hybrid demonstrated promising binding affinities toward the BCL-2 protein structure 4LVT, with docking scores of −7.1 kcal mol^{-1} on chain A and −7.8 kcal mol^{-1} on chain B. These values indicate a moderate to strong binding potential, particularly on chain B, where the energy interaction was more favorable. The difference in scores between the two chains can be attributed to subtle conformational differences in the binding grooves or the flexibility of side chains surrounding the active site.

On chain B, the hybrid likely achieved deeper penetration into the BH3-binding groove, forming stabilizing interactions

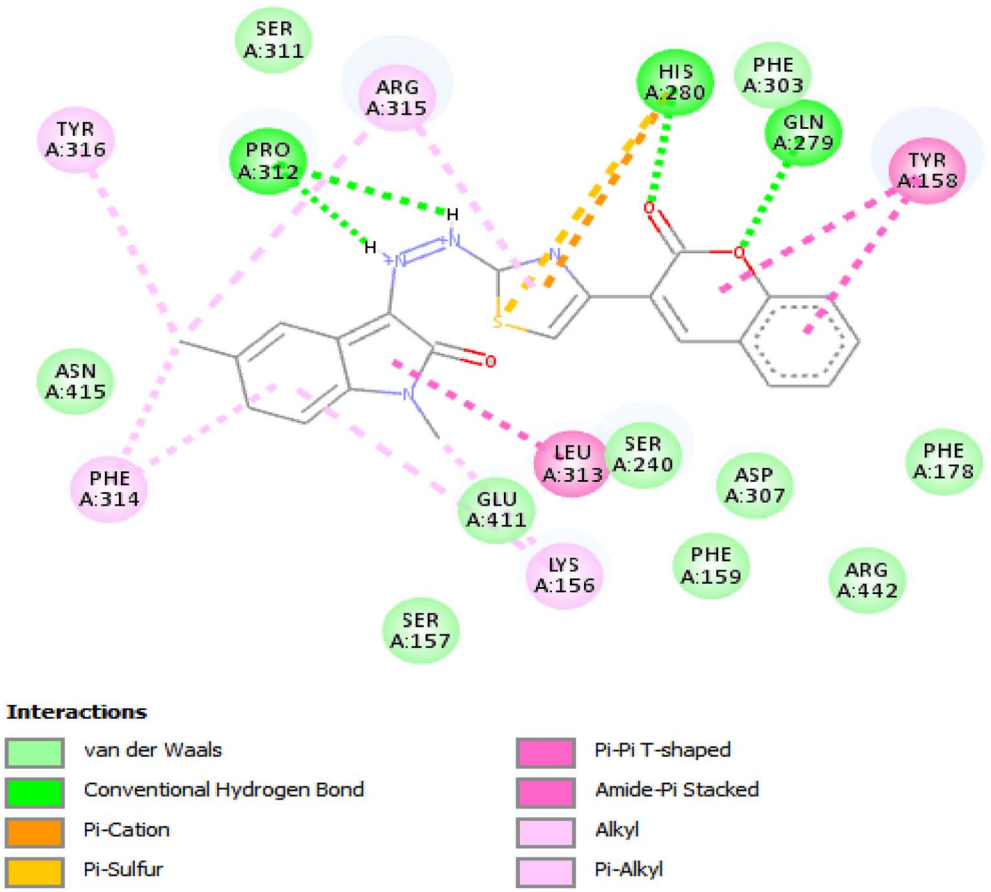

Fig. 12 Illustrative 2D models showing the interaction between the hybrid **5** and 3aj7 protein receptor.

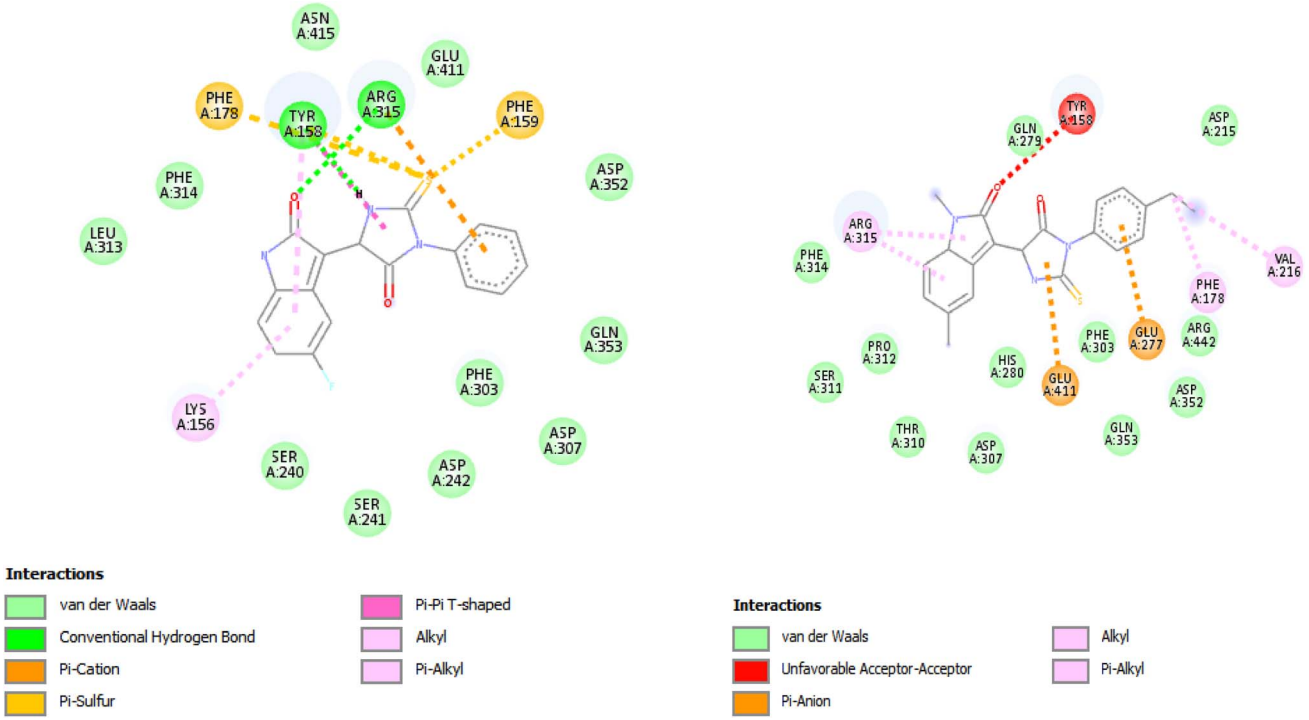

Fig. 13 Illustrative 2D models showing the interaction between hybrid **9** and **10** with the 3aj7 protein receptor.

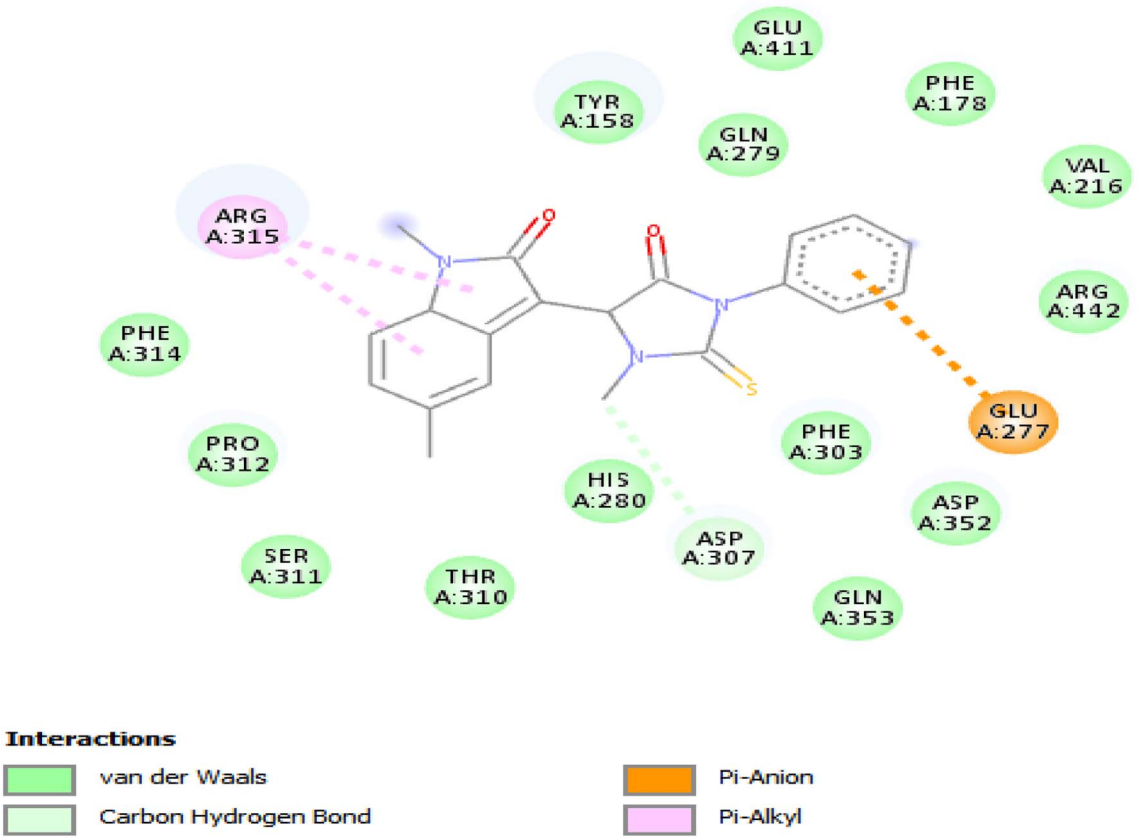

Fig. 14 2D illustration of interaction between the hybrid **12** and 3aj7 protein receptor.

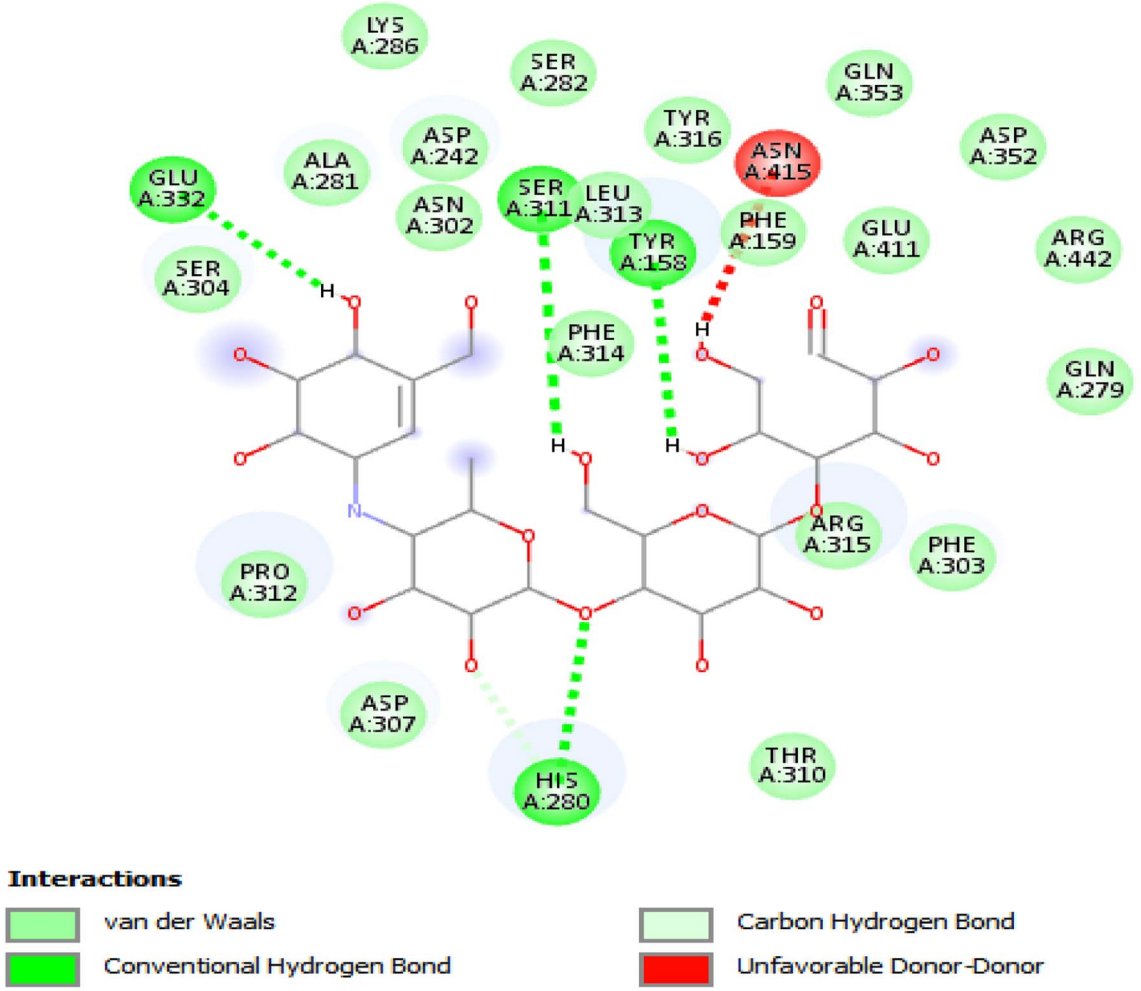

Fig. 15 Illustrative 2D models showing the interaction between acarbose and 3aj7 protein receptor.

with key residues, which are known to play critical roles in ligand recognition and stabilization. The isatin moiety, acting as a core anchoring group, while the coumarin ring system contributes to π–π stacking and hydrophobic interactions, enhancing binding affinity. In contrast, on chain A, the slightly lower docking score suggests a marginally less optimal alignment, possibly due to steric hindrance or minor shifts in residue orientation. Fig. 10 and 11.

Overall, the observed docking scores support the potential of the isatin–coumarin hybrid as a BCL-2 inhibitor, with a particularly favorable interaction profile on chain B. These findings highlight the importance of considering protein multimeric states and chain-specific interactions during inhibitor design. Table 5.

From the docking data.

• The isatin core is a key pharmacophore, anchoring within the hydrophobic cleft.

• The thiazole/thiohydantoin extensions likely improve hydrogen bonding and polar interactions.

• Coumarin ring increases π–π stacking and hydrophobic contact, enhancing affinity.

2.4.2. Implications for apoptosis induction. Since BCL-2 overexpression contributes to cancer cell resistance to apoptosis, effective inhibition can restore the apoptotic pathway. The promising docking profiles of the synthesized hybrids suggest their potential to act as BH3-mimetic agents, capable of disrupting BCL-2-mediated survival signaling.

2.4.3. Alpha-glucosidase activity. PDB ID: 3AJ7 corresponds to human maltase-glucoamylase, an important enzyme in carbohydrate metabolism. It's a target for type 2 diabetes treatment, since it breaks down complex carbohydrates into glucose. Acarbose is a known inhibitor of this enzyme, so comparing the synthesized hybrids to acarbose makes sense pharmacologically. Hybrid **5** appears to bind effectively in the catalytic pocket of 3AJ7, forming: hydrogen bonds (with residues like SER A:240, GLU A:411), π–π and π-π-cation interactions (with PHE, HIS, and ARG residues), and Pi–sulfur interaction, possibly from the thiazole moiety. These interactions help anchor the ligand, suggest stereoelectronic complementarity, and likely contribute to stability and inhibition Fig. 12–14.

2.4.4. Comparison to acarbose. Acarbose mainly forms hydrogen bonds due to its polar nature. Isatin hybrids, by

Table 6 Docking score of synthesized compounds with 3AJ7

Ligands	Binding energy (kcal mol^{-1})
5	−11
9	−10.5
10	−9.9
12	−10
Acarbose	−7.8

contrast, show diverse interactions, including aromatic π-systems and hydrophobic interactions. This could mean better membrane permeability, more specific binding, and potentially reduced off-target effects Fig. 15. Docking score shown in Table 6.

2.4.5. Anticholinesterase activity. The molecular docking study of the designed isatin-based hybrids with human acetylcholinesterase (AChE, PDB ID: 4PQE) revealed a favorable binding profile within the enzyme's active site. The hybrid **5** exhibited several key interactions: a hydrogen bond with TYR510 and π–π-cation interaction with ARG524, which lies near the choline-binding pocket, anchoring the aromatic moiety of the compound. Additional hydrogen bonds were formed with GLY523, GLN527, and ALA526–528, which contribute to the stabilization of the ligand within the binding gorge. Hydrophobic contacts with VAL330, VAL408, and LYS332 further enhance binding affinity through Pi–alkyl interactions. These interactions suggest that the compound may effectively block substrate access to the catalytic triad, mimicking the behavior of known AChE inhibitors such as donepezil. The observed binding features underscore the hybrid's prospect as a promising anticholinesterase agent for further pharmacological evaluation. The hybrid **10** exhibited multiple van der Waals interactions with key residues such as LEU540, LEU536, TRP532, THR238, and GLY234, suggesting that the compound fits moderately well within the enzyme's binding pocket. Additionally, halogen bonding (fluorine-mediated) interactions were observed with ASN533, PRO410, and CYS409, which are often critical for enhancing binding affinity and specificity in halogenated ligands. However, no classical hydrogen bonding or π–π stacking interactions (*e.g.*, with TRP84 or PHE330 common in potent AChE inhibitors) were observed, indicating a lack of strong anchoring to the catalytic triad or peripheral anionic site

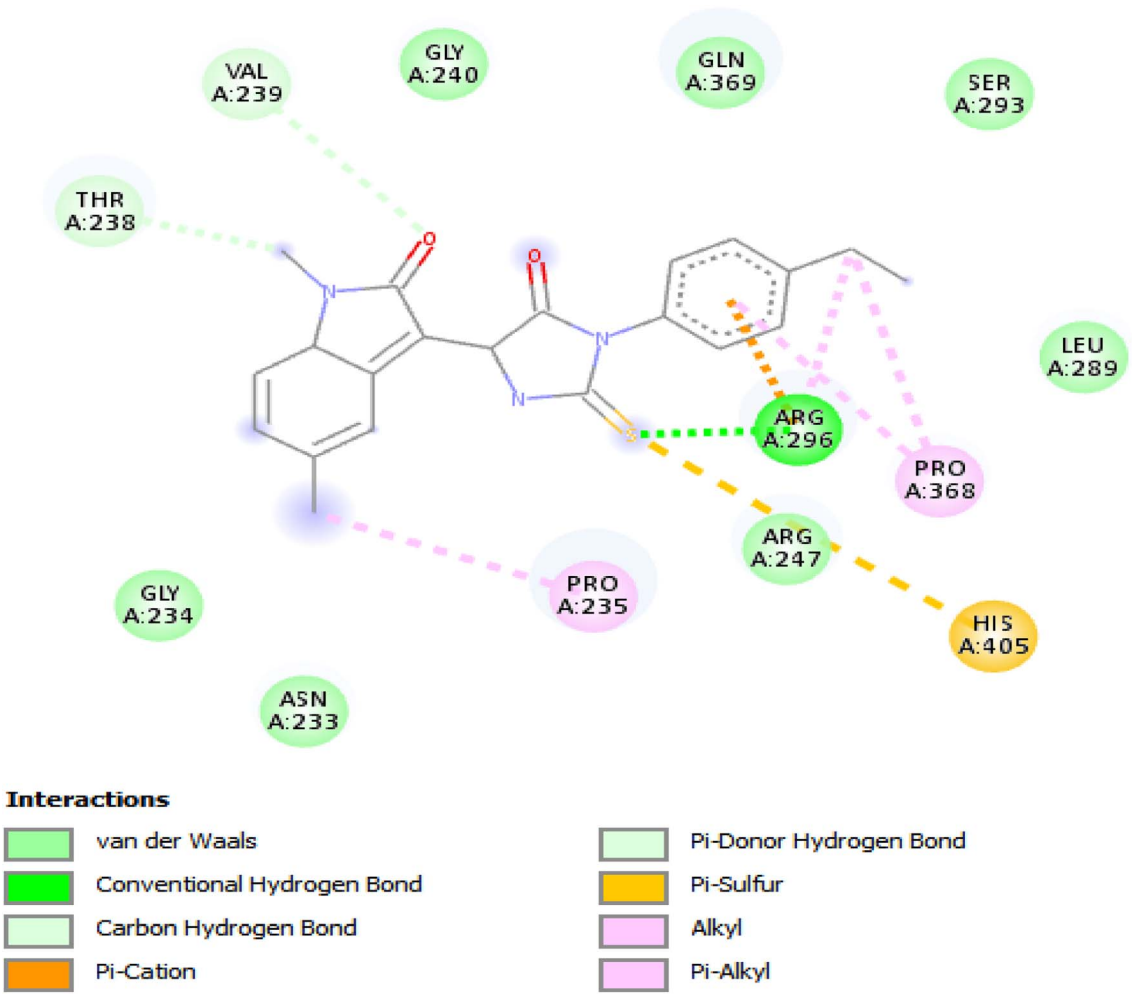

Fig. 16 2D illustration of interaction between the hybrid **9** and 4pqe protein receptor.

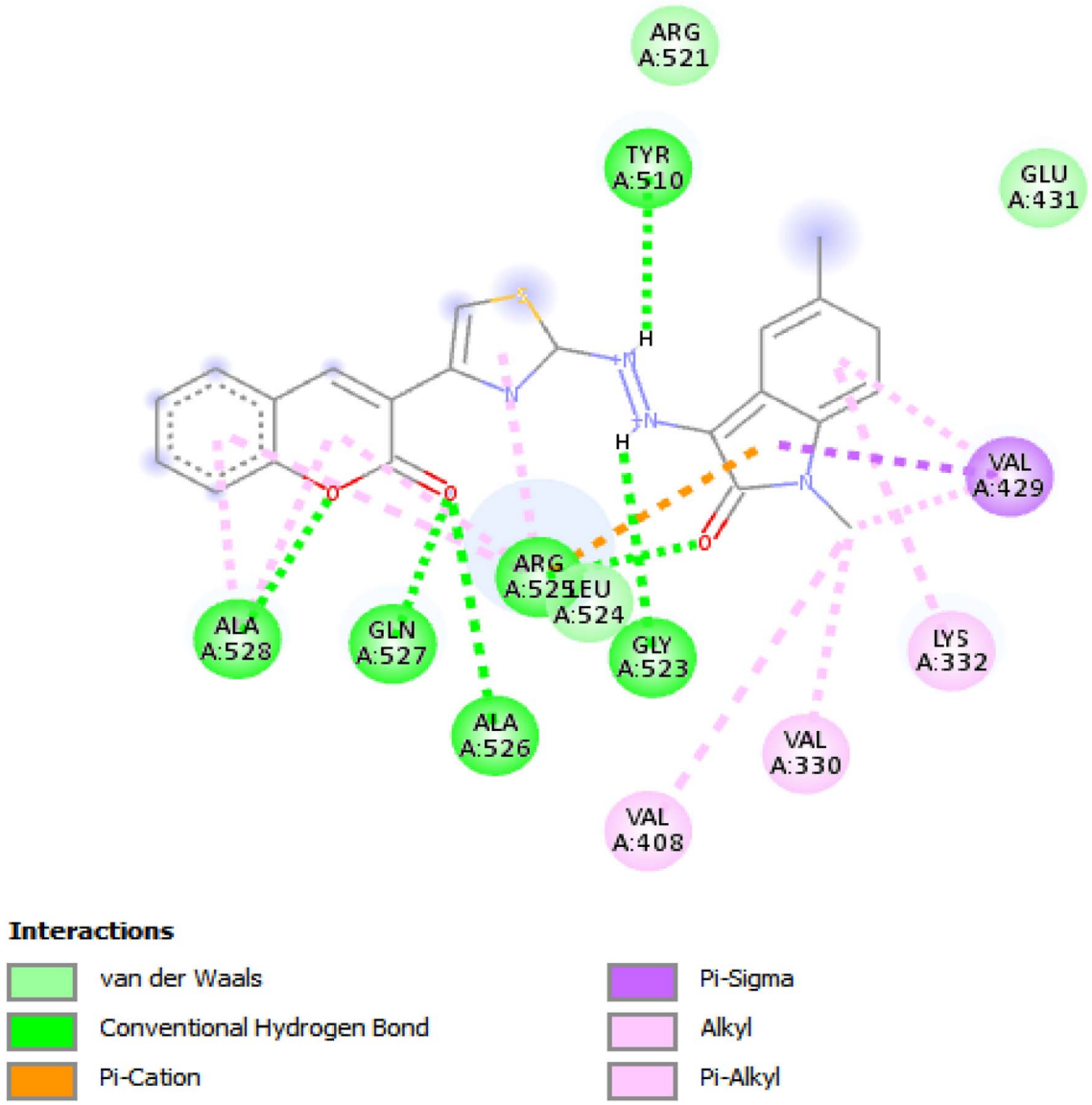

Fig. 17 2D illustration of interaction between the hybrid **5** and 4pqe protein receptor.

of the enzyme. Fig. 16–18 this supports the conclusion that the compound does not favorably interact with the key residues responsible for AChE inhibition. Table 7.

2.4.6. Anti-MRSA activity. The hybrid **10** exhibits strong and specific interactions with the binding pocket of PBP2a (PDB ID: 1MWT), suggesting potential as a promising anti-MRSA agent. The following interactions were observed: the combination of hydrogen bonding, electrostatic, and π-interactions across multiple key residues suggests this ligand has high potential for inhibiting PBP2a Tables 8–10. These findings support its further development as an anti-MRSA therapeutic candidate. Fig. 19–21.

Based on the previous comparison, hybrid **10** demonstrates a stronger and more diverse interaction profile, including direct contact with the catalytic serine (SER643), making it a more promising candidate for PBP2a inhibition and potential anti-MRSA activity.

3. Conclusion

This synthetic strategy provides a straightforward and efficient green route to novel isatin–thiohydantoin hybrids using readily available starting materials and environmentally friendly conditions (ethanol as solvent). The Knoevenagel condensation plays a key role in introducing structural rigidity and conjugation into the final molecules, which may improve their pharmacological potential. Overall, the combined biological evaluation and molecular docking studies clearly show that compound **5** is the most promising candidate in this series. It consistently performed better than all other tested derivatives in the enzymatic inhibition assays. It had the lowest IC_{50} value against AChE, demonstrated superior antimicrobial activity, and exhibited favorable antibiofilm effects. Additionally, molecular docking revealed strong binding affinity and good interactions within the enzyme active site,

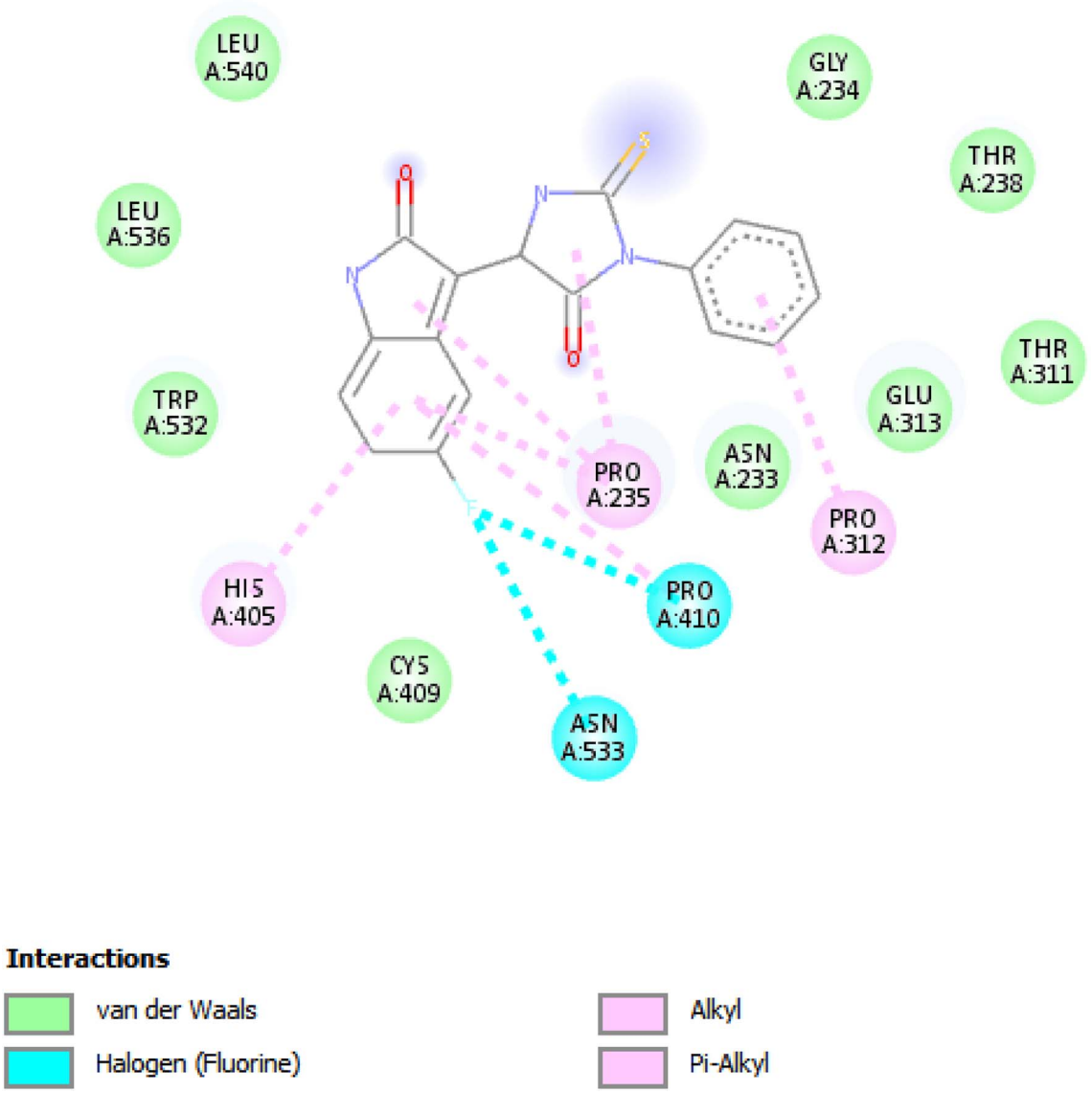

Fig. 18 2D illustration of interaction between the hybrid **10** and 4pqe protein receptor.

Table 7 Docking score of synthesized compounds with 4PQE

Ligands	Binding energy (kcal mol^{-1})
5	−8.6
9	−8.2
10	−8.1
12	−6.5
Donepezil	−8.3

Table 8 Docking score of synthesized compounds with 1mwt

Ligands	Binding energy (kcal mol^{-1})
5	−7.8
9	−5.9
10	−7.1
12	−6.5
Donepezil	−6.5

supporting the experimental results. These findings highlight compound **5** as a powerful, multifunctional scaffold with significant potential for further development as a therapeutic lead.

4 Experimental section

4.1 Synthesis of (Z)-5-chloro-1-methyl-3-(2-(5-(2-oxo-2H-chromen-3-yl)thiazol-2-yl)hydrazono)indolin-2-one 5 (ref. 32)

Thiosemicarbazide **13** is reacted with 3-(2-bromoacetyl)-2H-chromen-2-one (1.25 g, 5 mmol) (**4**) under reflux in ethanol to afford a 2-substituted thiazol-4-yl hydrazine derivative. Thiazolyl hydrazine is then refluxed with 5-chloroisatin in ethanol to yield isatin–thiazole coumarin hydrazone **5**.

Table 9 Interaction of hybrid 5 with 1mwt receptor

Ligand interaction	Pocket residue	Significance
Π-cation	HIS583	Strong electrostatic + stacking interaction with aromatic moieties. Stabilizes ligand
π-anion	ASP586	Electrostatic interaction with negatively charged side chain. Boosts binding affinity
Hydrogen bond	SER643	Anchors ligand and may block catalytic serine
Hydrogen bond	GLU585	Directional H-bond, contributes to specificity
Hydrogen bond	THR582	Anchoring and orientation of ligand
π–π stacking	HIS583	Aromatic stacking interaction. Enhances ligand stability and orientation

Table 10 Comparison between hybrid 5 and hybrid 10 interaction with 1mwt receptor

Interaction type	Hybrid **10**	Hybrid **5**
Hydrogen bonds	SER643, GLU585, THR582 (strong, directional)	None
Electrostatic interactions	π-cation (HIS583), π-anion (ASP586)	Attractive charge (GLU447)
Aromatic interactions	π–π with HIS583	π–π with TYR446
Hydrophobic interactions	Nonspecific	Alkyl/π-alkyl (HIS583), π-sigma (LYS581)
Targeting catalytic residues	Yes (direct interaction with SER643)	No direct targeting

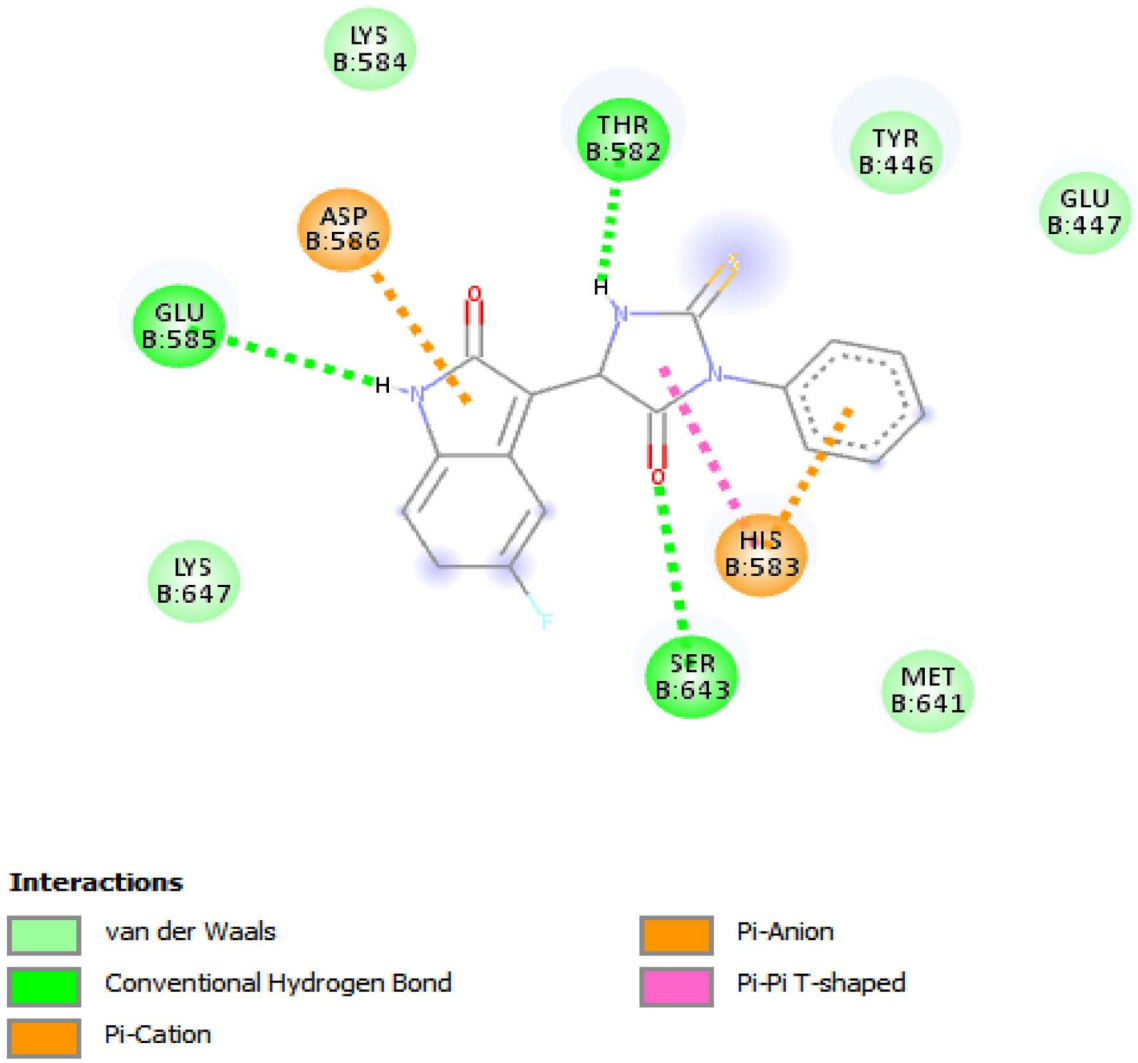

Fig. 19 2D illustration of interaction between the hybrid 10 and 1mwt protein receptor.

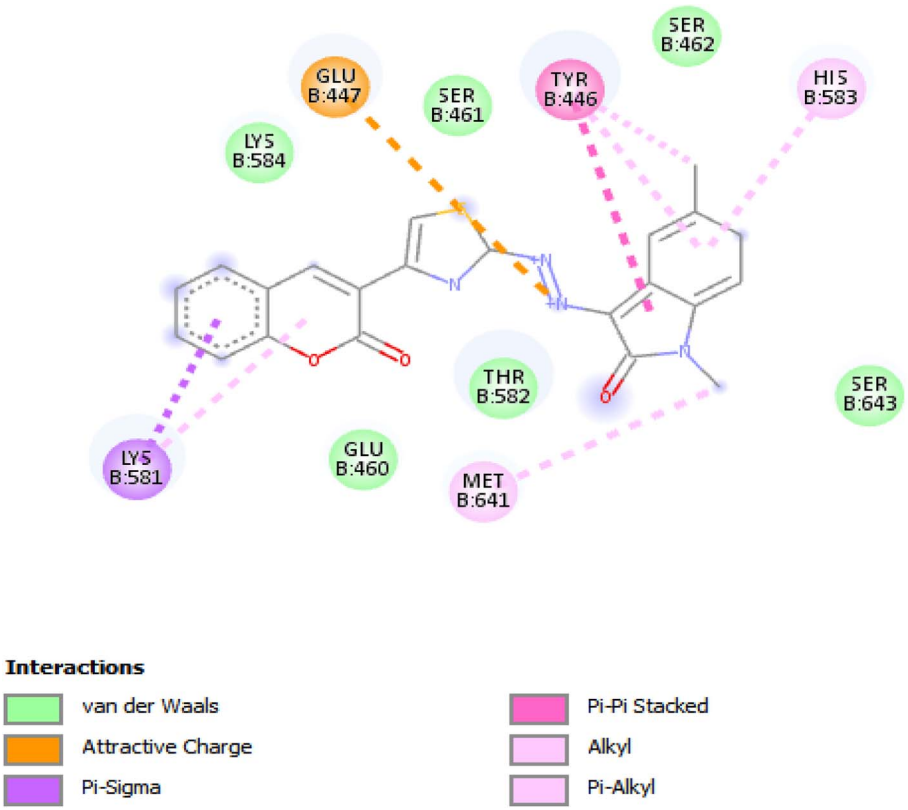

Fig. 20 2D illustration of interaction between the hybrid **5** and 1mwt protein receptor.

4.2 (Z)-5-Chloro-1-methyl-3-(2-(5-(2-oxo-2H-chromen-3-yl) thiazol-2 yl)hydrazono)indolin-2-one 5

Canary yellow crystals, m.p 258–260 °C, yield 90%. FTIR: ν max per cm^{-1}3 383, 3052, 2946, 2842, 1720, 1694, 1550, 1205, 808, 748.^{1}H NMR (400 MHz, DMSO) δ 11.06 (s, 1H), 8.66 (s, 1H), 8.44 (s, 1H), 7.85 (dd, J = 7.5, 3.4 Hz, 1H), 7.75–7.64 (m, 1H), 7.50 (d, J = 10.1 Hz, 2H), 7.43 (d, J = 7.5 Hz, 2H), 7.08 (d, J = 8.0 Hz, 1H), 3.20 (s, 3H). ^{13}C NMR (101 MHz, DMSO) δ 169.2, 163.8, 160.7, 153.7, 140.4, 139.1, 138.45, 135.4, 132.6, 131.1, 129.3, 128.7, 128.4, 128.1, 127.3, 126.3, 126.0, 120.9, 115.7, 113.7, 22.2. Analysis for $C_{21}H_{13}ClN_4O_3S$ (436.87): calcd (%) C 57.74; H 3.00; N 12.82; observed C 57.96; H 3.18; N 13.09.

4.3 Synthesis of 5-cloro-isatin-hydantion hybrid[33]

A solution of **hydantoin** (1 equiv.) was prepared in ethanol. To this solution, 5-fluoro isatin or 5-chloroisatin (1 equiv.) was added, and the reaction mixture was refluxed for 2 h. The progress of the reaction was monitored by TLC. The resulting precipitate was collected by filtration, washed with cold water, followed by cold diethyl ether, and then dried.

4.3.1 (Z)-5-chloro-3-(1-(4-ethylphenyl)-5-oxo-2-thioxoimidazolidin-4-ylidene)-1-methylindolin-2-one 9. Yellowish red crystals, m.p 265–267 °C, yield 92%. FTIR: ν max per cm^{-1}3 293, 3070, 2956, 2862, 1720, 1696, 1555, 1207, 820, 747.^{1}H NMR (400 MHz, DMSO) δ 9.89 (s, 1H), 8.65 (d, J = 8.8 Hz, 1H), 8.02 (d, J = 8.5 Hz, 2H), 7.98 (d, J = 2.7 Hz, 1H), 7.61 (d, J = 8.5 Hz, 2H), 7.38 (dd, J = 8.8, 2.7 Hz, 1H), 3.54 (s, 3H), 1.99–1.49 (m, 2H), 1.05 (t, J = 7.0 Hz, 3H). ^{13}C NMR (101 MHz, DMSO) δ 174.0, 168.5, 163.6, 140.1, 136.9, 134.4, 131.1, 130.1, 130.1, 129.3, 127.7, 126.0, 120.5, 56.5, 23.6, 19.0. Analysis for $C_{20}H_{16}ClN_3O_2S$ (397.87): calcd (%) C 60.38; H 4.05; N 10.56; observed C 60.27; H 4.23; N 10.68.

4.3.2 (Z)-5-chloro-3-(5-oxo-1-phenyl-2-thioxoimidazolidin-4-ylidene)indolin-2-one 10. Yellowish red crystals, m.p 265–267 °C, yield 92%. FTIR: ν max per cm^{-1}3 469, 3393, 3076, 2986, 2852, 1720, 1648, 1581, 1226, 860, 758.^{1}H NMR (400 MHz, DMSO) δ 11.72 (s, 1H), 11.24 (s, 1H), 8.55 (s, 1H), 7.61–7.51 (m, 3H), 7.46 (d, J = 7.9 Hz, 2H), 7.38 (d, J = 8.4 Hz, 1H), 6.97 (d, J = 8.4 Hz, 1H). ^{13}C NMR (101 MHz, DMSO) δ 174.0, 168.50, 163.5, 140.1, 136.9, 134.4, 131.0, 130.1, 129.5, 129.2, 129.2, 128.8, 127.6, 126.0, 120.5. Analysis for $C_{17}H_{10}FN_3O_2S$ (339.34): calcd (%) C 60.17; H 2.97; N 11.81; observed C 60.45; H 3.12; N 11.51.

4.3.3 (Z)-5-chloro-1-methyl-3-(3-methyl-5-oxo-1-phenyl-2-thioxoimidazolidin-4-ylidene)indolin-2-one 12. Red crystals, m.p 275–277 °C, yield 89%. FTIR: ν max per cm^{-1}3 095, 2996, 2872, 1715, 1642, 1585, 1221, 853, 765.^{1}H NMR (400 MHz, DMSO) δ 8.34 (d, J = 5.3 Hz, 1H), 7.74 (d, J = 8.0 Hz, 1H), 7.62 (s, 1H), 7.50–7.33 (m, 2H), 7.24–7.02 (m, 2H), 6.90 (s, 1H), 3.86 (s, 3H), 3.17 (s, 3H). ^{13}C NMR (101 MHz, DMSO) δ 174.1, 168.5,

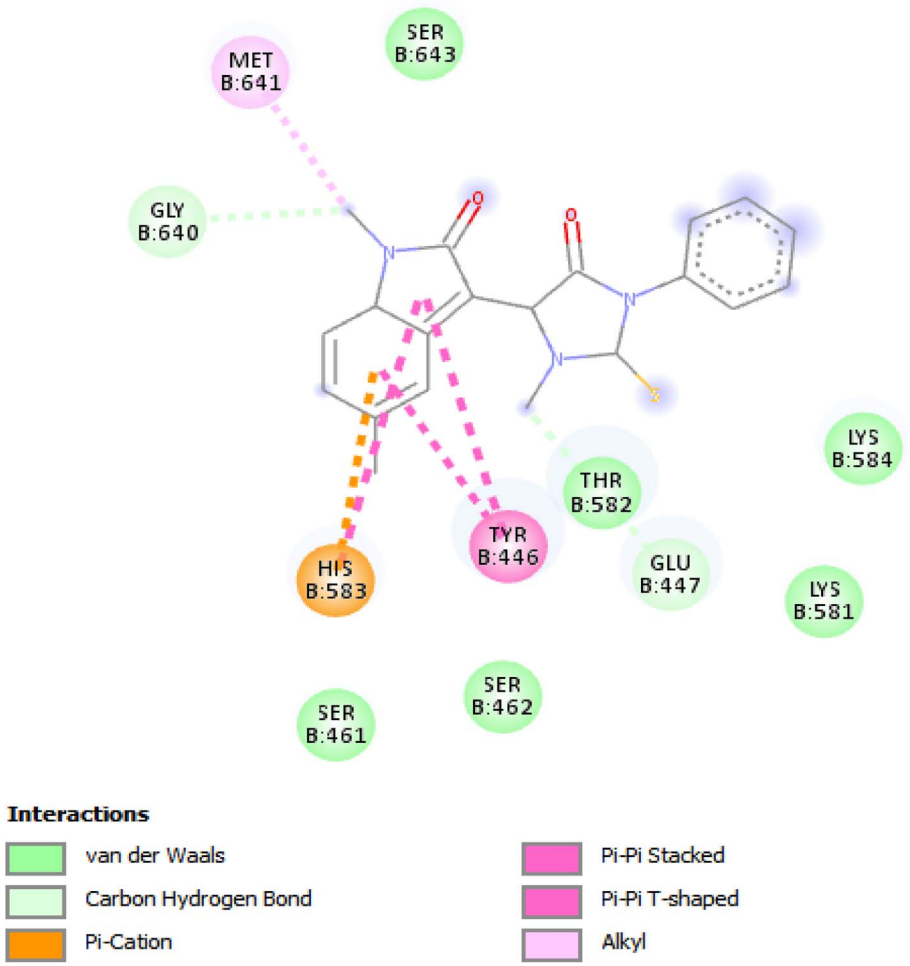

Fig. 21 2D illustration of interaction between the hybrid **9** and 1mwt protein receptor.

163.7, 140.1, 136.9, 134.4, 131.2, 130.2, 129.5, 129.2, 127.6, 126.1, 120.6, 23.7, 19.1. Analysis for $C_{19}H_{14}ClN_3O_2S$ (383.85): calcd (%) C 59.45; H 3.68; N 10.95; observed C 59.68; H 3.80; N 11.01.

Biological studies

The procedures for biological studies are mentioned in the SI file.

Conflicts of interest

There are no conflicts of interest to declare.

Data availability

All data supporting the findings of this study are available within the article and its SI file.

All experimetal files, raw data of the biological studies, and full description of methodology for the biological part. See DOI: **https://doi.org/10.1039/d5ra04722f**.

References

1 L. Szablewski, Associations Between Diabetes Mellitus and Neurodegenerative Diseases, *Int. J. Mol. Sci.*, 2025, **26**, 542, DOI: **10.3390/ijms26020542**.

2 G. D. Dimitriadis, P. Tessari, V. L. W. Go and J. E. Gerich, α-Glucosidase inhibition improves postprandial hyperglycemia and decreases insulin requirements in insulin-dependent diabetes mellitus, *Metabolism*, 1985, **34**, 261–265, DOI: **10.1016/0026-0495(85)90010-1**.

3 A. Bhushan, A. Gonsalves and J. U. Menon, Current State of Breast Cancer Diagnosis, Treatment, and Theranostics, *Pharmaceutics*, 2021, **13**, 723, DOI: **10.3390/pharmaceutics13050723**.

4 A. A. Jarrahpour and D. Khalili, Synthesis of 3-[(4-{3-[(2-oxo-1,2-dihydro-3H-indol-3-yliden)amino]phenoxy}phenyl) imino]-1H-indol-2-one as a novel Schiff base, *Molbank*, 2005, **2005**, M429, DOI: **10.3390/M429**.

5 H. Nazir and M. M. Naseer, The Isatin Scaffold: Exceptional Potential for the Design of Potent Bioactive Molecules, *Synlett*, 2025, DOI: **10.1055/a-2595-6787**.

6 S. Chowdhary, S. Shalini, A. Arora and V. Kumar, A Mini Review on Isatin, an Anticancer Scaffold with Potential Activities against Neglected Tropical Diseases (NTDs), *Pharmaceuticals*, 2022, **15**, 536, DOI: 10.3390/ph15050536.

7 I. A. Seliem, Synthesis, cytotoxic activity, molecular docking, molecular dynamics simulations, and ADMET studies of novel spiropyrazoline oxindoles based on domino Knoevenagel-Michael cyclization as potent non-toxic anticancer agents targeting β-tubulin and EGFR, with anti-MRSA activity, *RSC Adv.*, 2025, **15**, 20495–20512, DOI: 10.1039/d5ra01257k.

8 A. N. Kumar, S. R. Das, J. K. Kumar, K. V. N. S. Srinivas and S. D. Tetali, Design and development of an isatin-1,2,3-triazole hybrid analogue as a potent anti-inflammatory agent with enhanced efficacy and gene expression modulation, *RSC Adv.*, 2025, **15**, 2023–2033, DOI: 10.1039/d4ra07294d.

9 Z. Chen, Y. Guo, Y. Peng, X. Tan, H. Chen, D. Luo, K. Luo, D. Wu, Z. Huang, Z. Yu and C. Tao, Synthesis and biological evaluation of novel isatin-phenol hybrids as potential antitumor agents, *Bioorg. Chem.*, 2025, **157**, 108232, DOI: 10.1016/j.bioorg.2025.108232.

10 V. K. R. Tangadanchu, Y.-F. Sui and C.-H. Zhou, Isatin-derived azoles as new potential antimicrobial agents: Design, synthesis and biological evaluation, *Bioorg. Med. Chem. Lett.*, 2021, **41**, 128030, DOI: 10.1016/j.bmcl.2021.128030.

11 T. Elsaman, M. S. Mohamed, E. M. Eltayib, H. A. Abdel-aziz, A. E. Abdalla, M. U. Munir and M. A. Mohamed, Isatin derivatives as broad-spectrum antiviral agents: the current landscape, *Med. Chem. Res.*, 2022, **31**, 244–273, DOI: 10.1007/s00044-021-02832-4.

12 A. Oguz, A. Uysal, B. N. S. Özkan, M. Oguz and M. Yilmaz, Isatin-modified Calixarene derivatives: A comprehensive study on synthesis, enzyme inhibition, antioxidant, antimicrobial, and Antiproliferative activities, *Bioorg. Chem.*, 2025, **157**, 108280, DOI: 10.1016/j.bioorg.2025.108280.

13 S. Mehreen, M. I. Ali, S. tul Muntha, M. Zia, A. Ullah, S. Ullah, A. Khan, J. Hussain, M. U. Anwar, A. Al-Harrasi and M. M. Naseer, Synthesis, structural insights and bio-evaluation of N-phenoxyethylisatin hydrazones as potent α-glucosidase inhibitors, *RSC Adv.*, 2025, **15**, 14717–14729, DOI: 10.1039/d5ra00770d.

14 S. K. Bhattacharya, A. Clow, A. Przyborowska, J. Halket, V. Glover and M. Sandler, Effect of aromatic amino acids, pentylenetetrazole and yohimbine on isatin and tribulin activity in rat brain, *Neurosci. Lett.*, 1991, **132**, 44–46, DOI: 10.1016/0304-3940(91)90429-W.

15 S. Khatoon, R. Asif, S. Kalsoom, A. Aroosh, A. Islam, S. S. Tariq, Z. Ul-Haq and M. M. Naseer, Novel thiosemicarbazones of coumarin incorporated isatins: synthesis, structural characterization and antileishmanial activity, *J. Biomol. Struct. Dyn.*, 2025, 1–13, DOI: 10.1080/07391102.2025.2498072.

16 Moamen Hassanin, M. Mustafa, Eman Beshr, H. Hassan and O. Aly, Hydantoin derivatives: A review on their anticancer activities, *Octahedron Drug Res*, 2024, **4**(1), 61–74, DOI: 10.21608/odr.2023.232555.1029.

17 S. A. Patil, A. R. Nesaragi, R. R. Rodríguez-Berrios, S. M. Hampton, A. Bugarin and S. A. Patil, Coumarin Triazoles as Potential Antimicrobial Agents, *Antibiotics*, 2023, **12**, 160, DOI: 10.3390/antibiotics12010160.

18 A. Ibrar, Y. Tehseen, I. Khan, A. Hameed, A. Saeed, N. Furtmann, J. Bajorath and J. Iqbal, Coumarin-thiazole and -oxadiazole derivatives: Synthesis, bioactivity and docking studies for aldose/aldehyde reductase inhibitors, *Bioorg. Chem.*, 2016, **68**, 177–186, DOI: 10.1016/j.bioorg.2016.08.005.

19 S. Ramos-Inza, C. Aydillo, C. Sanmartín and D. Plano, Thiazole Moiety: An Interesting Scaffold for Developing New Antitumoral Compounds, in, *Heterocycles – Synthesis and Biological Activities*, IntechOpen, 2020, DOI: 10.5772/intechopen.82741.

20 I. A. Seliem, DMF-DMA catalyzed Synthesis, molecular docking, in-vitro, in-silico design, and binding free energy studies of novel thiohydantoin derivatives as antioxidant and antiproliferative agents targeting EGFR tyrosine kinase and aromatase cytochrome P450 enzyme, *Bioorg. Chem.*, 2024, **150**, 107601, DOI: 10.1016/j.bioorg.2024.107601.

21 H. Sun, M. F. Ansari, B. Fang and C.-H. Zhou, Natural Berberine-Hybridized Benzimidazoles as Novel Unique Bactericides against *Staphylococcus aureus*, *J. Agric. Food Chem.*, 2021, **69**, 7831–7840, DOI: 10.1021/acs.jafc.1c02545.

22 V. Gupta and P. Datta, Next-generation strategy for treating drug resistant bacteria, *Indian J. Med. Res.*, 2019, **149**, 97–106, DOI: 10.4103/ijmr.IJMR_755_18.

23 C. K. Jadhav, A. S. Nipate, A. V. Chate, V. D. Songire, A. P. Patil and C. H. Gill, Efficient Rapid Access to Biginelli for the Multicomponent Synthesis of 1,2,3,4-Tetrahydropyrimidines in Room-Temperature Diisopropyl Ethyl Ammonium Acetate, *ACS Omega*, 2019, **4**, 22313–22324, DOI: 10.1021/acsomega.9b02286.

24 A. I. Almansour, N. Arumugam, R. S. Kumar, R. Raju, K. Ponmurugan, N. AlDhabi and D. Premnath, Broad spectrum antimicrobial activity of dispirooxindolopyrrolidine fused acenaphthenone heterocyclic hybrid against healthcare associated microbial pathogens (HAMPs), *J. Infect. Public Health.*, 2020, **13**, 2001–2008, DOI: 10.1016/j.jiph.2020.09.016.

25 N. Nivetha and A. Thangamani, Dispirooxindole-pyrrolothiazoles: Synthesis, anti-cancer activity, molecular docking and green chemistry metrics evaluation, *J. Mol. Struct.*, 2021, **1242**, 130716, DOI: 10.1016/j.molstruc.2021.130716.

26 G. L. Ellman, K. D. Courtney, V. Andres and R. M. Featherstone, A new and rapid colorimetric determination of acetylcholinesterase activity, *Biochem. Pharmacol.*, 1961, **7**, 88–95, DOI: 10.1016/0006-2952(61)90145-9.

27 P.-L. Zhang, G. Lavanya, Y. Yu, B. Fang and C.-H. Zhou, Identification of a Novel Antifungal Backbone of Naphthalimide Thiazoles with Synergistic Potential for

Chemical and Dynamic Treatment, *Future Med. Chem.*, 2021, **13**, 2047–2067, DOI: **10.4155/fmc-2021-0162**.

28 K. M. Craft, J. M. Nguyen, L. J. Berg and S. D. Townsend, Methicillin-resistant *Staphylococcus aureus* (MRSA): antibiotic-resistance and the biofilm phenotype, *Medchemcomm*, 2019, **10**, 1231–1241, DOI: **10.1039/C9MD00044E**.

29 F.-F. Li, P.-L. Zhang, V. K. R. Tangadanchu, S. Li and C.-H. Zhou, Novel metronidazole-derived three-component hybrids as promising broad-spectrum agents to combat oppressive bacterial resistance, *Bioorg. Chem.*, 2022, **122**, 105718, DOI: **10.1016/j.bioorg.2022.105718**.

30 Y.-P. Xie, N. Sangaraiah, J.-P. Meng and C.-H. Zhou, Unique Carbazole-Oxadiazole Derivatives as New Potential Antibiotics for Combating Gram-Positive and -Negative Bacteria, *J. Med. Chem.*, 2022, **65**, 6171–6190, DOI: **10.1021/acs.jmedchem.2c00001**.

31 H. Sun, S.-Y. Huang, P. Jeyakkumar, G.-X. Cai, B. Fang and C.-H. Zhou, Natural Berberine-derived Azolyl Ethanols as New Structural Antibacterial Agents against Drug-Resistant *Escherichia coli*, *J. Med. Chem.*, 2022, **65**, 436–459, DOI: **10.1021/acs.jmedchem.1c01592**.

32 T. I. El-Emary, R. A. Ahmed and E. A. Bakhite, Synthesis of Some New Spiro, Isolated and Fused Heterocycles Based on 1 *H* -indole-2-One, *J. Chin. Chem. Soc.*, 2001, **48**, 921–927, DOI: **10.1002/jccs.200100134**.

33 M. Kukushkin, V. Novotortsev, V. Filatov, Y. Ivanenkov, D. Skvortsov, M. Veselov, R. Shafikov, A. Moiseeva, N. Zyk, A. Majouga and E. Beloglazkina, Synthesis and Biological Evaluation of S-, O- and Se-Containing Dispirooxindoles, *Molecules*, 2021, **26**, 7645, DOI: **10.3390/molecules26247645**.